

# MODELING OF HYDROGEN UPHILL DIFFUSION IN DISSIMILAR TITANIUM WELDS

Todd S. Mintz and Xihua He  
Center for Nuclear Waste Regulatory Analyses  
Southwest Research Institute®  
6220 Culebra Road  
San Antonio, Texas 78238

## ABSTRACT

Hydrogen embrittlement has been known to cause degradation in titanium alloys. The absorption of hydrogen into titanium can lead to the formation of brittle titanium hydrides, which decrease the fracture toughness of the metal. Weldments of dissimilar titanium alloys can be especially susceptible to hydride cracking. Experimental tests and field experiences have shown that hydrogen can diffuse to and accumulate on one side of the weldment. It is possible for hydrogen to diffuse to one of the welded alloys, even against a concentration gradient. This process, known as uphill diffusion, can occur because the chemical activity of hydrogen in the two welding metals may be different. One cause of the different activity is a difference in aluminum concentration between the two welded titanium alloys. Because hydrogen can undergo uphill diffusion, it can concentrate on one side of the weld leading to the formation of titanium hydrides and decreased fracture toughness. It has been proposed that uphill diffusion may be minimized if a fillet weld is used between the two dissimilar titanium welds. The fillet weldment, or transitional titanium alloy, would contain an aluminum concentration between the two welding materials. The objective of this work is to gain an understanding of how different titanium weld configurations, corrosion rates, and temperatures affect the hydrogen uphill diffusion process. Initially, laboratory testing was conducted to measure the corrosion rates of representative titanium alloys with 6 wt% and 0 wt% aluminum. These rates were then used in an uphill diffusion model. Using the measured corrosion rates, it was determined that a transition titanium alloy successfully reduced hydrogen concentration, but only at high temperatures  $\{>100\text{ }^{\circ}\text{C}\text{ [}212\text{ }^{\circ}\text{F}]\}$ . However, when the temperature was kept at  $25\text{ }^{\circ}\text{C}\text{ [}77\text{ }^{\circ}\text{F}]$ , the transition titanium alloy led to a higher maximum hydrogen concentration in the weldment.

## INTRODUCTION

Hydrogen can be detrimental to cracking resistance behavior of titanium and its alloys. This detrimental effect, known as hydrogen embrittlement, is attributed to the formation of brittle titanium hydrides, which can decrease the fracture toughness or ductility of the metal.<sup>1</sup> This leads to a decrease in the threshold stress required for cracking to occur. Hydrogen embrittlement can occur when the concentration of hydrogen reaches a critical level in the titanium alloy, allowing titanium hydrides to form.<sup>2,3</sup> Hydrogen embrittlement in titanium can be affected by a number of properties. One of these include the surrounding available hydrogen, which can be the natural environment or formed through corrosion processes.

The corrosion rate of titanium can influence the amount of hydrogen that absorbs into the titanium alloy. In some instances, the only sources of hydrogen may be the reaction of titanium with water as shown in Eq. (1)<sup>4</sup>



The reaction in Eq. (1) would be expected to occur on the TiO<sub>2</sub> surface under neutral pH conditions. This reaction will generate hydrogen that can be absorbed into the titanium matrix. The higher the corrosion rate, the more hydrogen can be generated.

One area where hydride cracking in titanium has been a concern is along the weld lines of dissimilar titanium alloys.<sup>5-6</sup> At dissimilar metal weldments, the hydrogen chemical activity can differ between the welded materials.<sup>5</sup> In such a case, there will be a driving force for the hydrogen to diffuse from one material to the other. The driving force may even lead to hydrogen diffusion up a concentration gradient (from lower concentration to higher concentration). The process where hydrogen may diffuse up a concentration gradient is called uphill diffusion, and this can lead to hydrogen segregation on one side of the weldments. If the hydrogen reaches the critical hydrogen concentration, hydrides will form and potentially lead to hydride cracking. Placing an intermediate fillet weld material with a hydrogen activity between the welded materials may reduce the diffusion of hydrogen across the dissimilar metal weld.<sup>5</sup>

Uphill diffusion has been studied to examine the effects of hydride cracking at dissimilar titanium metal weldments, particularly welds between Ti-6Al-4V and commercially pure titanium alloys, which are commonly used in industrial and commercial applications.<sup>6</sup> For instance, the weld of a forged Ti-6Al-4V pressure vessel catastrophically failed during a pressure test when commercially pure titanium was inadvertently used as the weld filler metal rather than Ti-6Al-4V. Subsequent analysis of the weld indicated that failure occurred due to hydride precipitation in the commercially pure titanium. Hydrogen segregation in the commercially pure titanium alloy was attributed to difference in aluminum content compared to the Ti-6Al-4V pressure vessel body, as an aluminum gradient may cause uphill diffusion (hydrogen will diffuse from the alloy containing higher aluminum content to the alloy containing lower hydrogen content).<sup>7</sup> It has been determined that the addition of aluminum to the titanium alloy increases the hydrogen activity, which provides the driving force for uphill diffusion<sup>5</sup>. The hydrogen diffusion in such a dissimilar titanium metal weldment can be evaluated using an uphill diffusion model.

The objective of this work was to examine factors influencing the uphill diffusion of hydrogen across a titanium dissimilar metal weldment. Initially, the corrosion rate of two titanium alloys was experimentally evaluated in a laboratory setting to gain an understanding of the amount of hydrogen that could be generated and used to form hydrides. Using this experimental data, an uphill diffusion model was created to examine the factors influencing uphill diffusion across dissimilar titanium metal weldment. The factors examined include temperature, titanium corrosion rate, and two-alloy weldment versus a three-alloy weldment (i.e. transition material). The following section describes the experimental and uphill diffusion modeling approach.

## TECHNICAL APPROACH

To determine the role of temperature, corrosion rate, and welding configuration on the hydrogen embrittlement of titanium alloys at a welding joint, titanium alloys with different aluminum content were experimentally tested and an uphill hydrogen diffusion model was developed based on the experimental results.

## Experimental Approach

Titanium Grades 7 and 29 were used to simulate titanium alloys with aluminum content of 0 and 6 wt%, respectively. Table 1 lists the chemical composition of Titanium Grades 7 and 29. Passive corrosion rates of Titanium Grades 7 and 29 were measured using electrochemical impedance spectroscopy at elevated temperatures. Limited potentiostatic polarization tests were performed on Titanium Grade 29 to measure the corrosion rates for comparison with that measured by electrochemical impedance spectroscopy. Test methods have been detailed previously.<sup>8,9</sup> Both electrochemical impedance spectroscopy and potentiostatic tests were conducted using cylindrical specimens of 6.3 mm [0.25 in] in diameter and 48.6 mm [1.91 in] in length. All specimens were polished to a 600-grit finish, cleaned ultrasonically in detergent, rinsed in deionized water, ultrasonically cleaned in acetone, and dried. At the completion of each test, the specimens were rinsed in deionized water and dried.

Tests were conducted in 2-L [0.53-gal] glass cells with polytetrafluoroethylene (PTFE) lids. The cells were fitted with a water-cooled condenser and a water trap to minimize solution loss at elevated temperatures and by air intrusion. The saturated calomel reference electrode was connected to the solution through a water-cooled Luggin probe with a porous silica tip, and the reference electrode was maintained at room temperature. A platinum flag was used as a counterelectrode. Solutions of 1 M NaCl and 4 M MgCl<sub>2</sub> were used in the test. All solutions were deaerated with high-purity nitrogen for at least 24 hours prior to the start of the tests.

Electrochemical impedance spectra were obtained at an open circuit over a frequency range of 100,000 to 0.001 Hz in 1 M NaCl and 4 M MgCl<sub>2</sub> solutions at temperatures of 30, 45, 60, 80, 95, and 110 °C [86, 113, 140, 176, 203, and 230 °F] sequentially {110 °C [230 °F] was only applied for tests conducted in 4 M MgCl<sub>2</sub> solution}. The tests were started at 30 °C [86 °F]. After the impedance measurement at each temperature, the solution was set to the next higher temperature and maintained at that temperature for 7–10 days. Duplicate tests were run for all temperatures. The spectra were fit to an analog equivalent circuit. The resistive component of the analog circuit was used to extract the polarization resistance,  $R_p$ , and calculate the corrosion current density,  $i_{corr}$ , using Eq. (2)

$$R_p = \frac{\beta_a \beta_c}{2.303(\beta_a + \beta_c)i_{corr}} \quad (2)$$

where

$\beta_a$  — anodic Tafel slope  
 $\beta_c$  — cathodic Tafel slope

For palladium- or ruthenium-containing titanium alloys, assuming the anodic Tafel slope to be infinite<sup>10</sup> and the cathodic Tafel slope to be –60 mV/decade,<sup>11</sup> the corrosion current density is calculated according to Eq. (3)

$$i_{corr} = \frac{\beta_c}{2.303R_p} \quad (3)$$

The corrosion rate can then be calculated using Eq. (4)

$$\text{Corrosion Rate (mm/yr)} = \frac{K i_{corr} EW}{\rho} \quad (4)$$

where

$EW$  — equivalent weight  
 $K$  — conversion factor  
 $\rho$  — density

For Titanium Grades 7 and 29,  $\rho$  is 4.50 and 4.42 g/cm<sup>3</sup> [281 and 276 lb/ft<sup>3</sup>]. Assuming dissolution of titanium to Ti<sup>4+</sup> and ignoring dissolution of other elements in Titanium Grade 7, the equivalent weight for Titanium Grade 7 is 12.0 g/mol.<sup>12</sup> Assuming congruent dissolution of the major alloying elements Ti<sup>4+</sup>, Al<sup>3+</sup>, and V<sup>5+</sup> at 0 mV<sub>SCE</sub>, the equivalent weight for Titanium Grade 29 is 11.6 g/mol.<sup>12</sup>

The anodic current density was measured in potentiostatic tests, and the Titanium Grade 29 specimens were maintained at a potential of 0 mV<sub>SCE</sub> and temperature of 95 °C [203 °F] for 60 days. At the conclusion of the test, the specimens were reweighed and examined for corrosion with an optical microscope. Corrosion rates were calculated using Eq. (4) based on the measured anodic current density.

#### Uphill Diffusion Model Approach

Hydrogen enrichment at a weld line, leading to hydrogen embrittlement, has been observed to occur in titanium welds.<sup>5,6</sup> The hydrogen segregation at the boundary between welded materials as been shown to be due to the welding process.<sup>5</sup> However, the diffusion of hydrogen that leads to the hydrogen embrittlement is not predicted by the original form of Fick's Law of diffusion.<sup>13</sup> The Fick's First Law for an isotropic material is given by Eq. (5)

$$J = -D \nabla C \quad (5)$$

where

$J$  — flux  
 $D$  — diffusivity  
 $C$  — hydrogen concentration

In the case of the hydrogen diffusion along the welding line of the titanium alloys, gradients other than hydrogen concentration can lead to a driving force for the movement of hydrogen. This type of diffusion was named "uphill diffusion."<sup>5-7</sup> In this paper, a one-dimensional, isotropic form of the Fick's First Law for uphill diffusion, given by Eq. (6), was used containing chemical potential gradient for aluminum and the chemical potential gradient of the diffusing hydrogen.<sup>6</sup> This paper did not examine the

effect of potential stress gradients or temperature gradients, which would both affect the uphill diffusion of hydrogen.

$$J = -D \left[ \frac{\partial C}{\partial x} + CK_a \frac{\partial N_a}{\partial x} \right] \quad (6)$$

In Eq. (6),  $K_a$  is an experimental constant (3.55),<sup>7</sup>  $N_a$  is the concentration of aluminum in the titanium alloy in ppm,  $C$  is concentration of hydrogen in ppm,  $x$  is distance in cm, and  $D$  is cm<sup>2</sup>/second. When Eq. (6) is converted to the form of Fick's Second Law, it results in the following equation.

$$\frac{\partial C}{\partial t} = D \left[ \frac{\partial^2 C}{\partial x^2} + K_a \frac{\partial C}{\partial x} \frac{\partial N_a}{\partial x} + K_a C \frac{\partial^2 N_a}{\partial x^2} \right] \quad (7)$$

Eq. (7) was numerically solved using finite difference methods. The space domain was partitioned using a mesh  $x_0, \dots, x_j$ , and the time domain was partitioned using a mesh  $t_0, \dots, t_N$ . The two consecutive points in space will be set at a value  $h$ , and the two consecutive points in time will be held at a value of  $k$ . The finite element method chosen to solve Eq. (7) was an implicit approach because it allows for the use of large time steps while achieving an accurate solution. This method was used to solve the hydrogen diffusion equation across a dissimilar titanium metal weldment while examining the influence of corrosion rate, temperature, and weld configuration.

One of the factors suggested to influence the diffusion of hydrogen at a dissimilar metal weldment is the weld configuration. In this study, two welding configurations were simulated, a two-alloy dissimilar titanium metal weldment and a three-alloy dissimilar metal weldment. The two-alloy dissimilar metal weldment consisted of welding two materials together. One material had a 6 wt% of aluminum, similar to Titanium Grade 29, while the other material had no aluminum, similar to Titanium Grade 7. The one-dimensional width for each alloy was equal and set at 38 cm [15 in] to provide a large distance for diffusion to occur. The second type of weld joint configuration examined consisted of three titanium alloys welded together. This included a titanium alloy containing 6 wt% of aluminum welded to an alloy containing 3 wt% of aluminum, which was finally welded to an alloy containing no aluminum. The one-dimensional width for each alloy on the outer sides of the welding configuration was 38 cm [15 in]. The interior alloy (i.e., transition alloy) one-dimensional width was held at 3 cm [1.2 in]. Figure 1 demonstrates the two different welding configurations examined. The thickness of the alloys was assumed to be 0.75 cm [0.30 in]. For modeling simplicity, it was assumed that any hydrogen absorbing into an alloy will uniformly distribute through the thickness of the alloy instantaneously. This allowed the diffusion process to be modeled one dimensionally. In addition, the boundary conditions at each end of the weldment established no diffusion of hydrogen out of the given weldment (diffusion at each boundary was zero). To insure this did not affect the diffusion results along the boundary between welded materials, the width of the outer weldment material was made large. The results will show that boundary condition did not affect the outcome of the model simulations.

As mentioned previously, the corrosion rate was one factor examined in the present study. The corrosion rate directly determines the amount of hydrogen formed that can

be used to embrittle the titanium alloy. In the current model, it was assumed that the only source of hydrogen was the corrosion reaction of titanium with water shown by Eq. (1). Higher corrosion rates will lead to the formation of more hydrogen, which can then be absorbed into the titanium. It was assumed for this model that the corrosion process would occur uniformly on one side of the weldment as shown in Figure 1. Secondly, it was decided to use a hydrogen adsorption efficiency of 1.5 percent.<sup>4</sup> Therefore, for all of the hydrogen formed by the corrosion reaction, only 1.5 percent would be absorbed into the titanium weldment.

The corrosion rate was examined by comparing two different conditions. The first condition examined was a constant corrosion rate. In this case, the corrosion rate for all titanium alloys was set to a value that lay within the range determined by the experimental studies. The second condition examined the condition where one of the alloys involved in the welding process had a higher corrosion rate. In the current form of the model, the titanium alloy with 0 wt% aluminum was held at the lower corrosion rate, while the other alloys had a corrosion rate that was roughly 3.5 times higher than the constant corrosion rate.

The last factor examined in the hydrogen diffusion model was temperature. As mentioned previously, no temperature gradient was examined. Instead, the absolute temperature was changed between 25 and 100 °C [77 and 212 °F]. The main change this has on the system is related to the diffusivity of hydrogen in titanium. Titanium alloys may contain mixed phases, which can have different hydrogen diffusivities. For this study, to simplify the mathematics, the simulated titanium alloys were assumed to be homogenous. The diffusivity of hydrogen in all the titanium alloys used was given as a function of temperature shown in Eq. (8)<sup>6</sup>

$$D = 0.018 \exp\left(\frac{-12,380}{RT}\right) \quad (8)$$

where

$R$  — universal gas constant (cal mol K<sup>-1</sup>)  
 $T$  — temperature

By changing the temperature, the diffusion of hydrogen in the titanium alloy will be either increased or decreased, and the effect on the hydrogen profile will be examined.

## RESULTS AND DISCUSSION

The results of the titanium corrosion rate experimental studies and the hydrogen uphill diffusion modeling simulations are presented in the following section. As mentioned previously, the corrosion rate measurements determined experimentally were used to support the hydrogen uphill diffusion modeling. The hydrogen uphill diffusion modeling evaluated the effects of weld configuration, corrosion rate, and temperature at a dissimilar metal weldment.

## Corrosion Rate Measurement

The electrochemical impedance spectra for Titanium Grade 29 were analyzed using the one-time constant analog model shown in Figure 2, which has components for the solution resistance,  $R_s$ , polarization resistance,  $R_p$ , and constant phase element, CPE. Fitting the spectra with an analogy circuit with two time constants; was also attempted, however, the fitting error was too high to derive any meaningful quantitative data. Results by fitting to the one-time constant for Titanium Grade 29 in 1 M NaCl solution are shown in Figure 3. Error bars for the corrosion rate were from the fitting errors. The corrosion rates varied from 0.1 to 3 nm/yr [ $3.9 \times 10^{-6}$  to  $1.2 \times 10^{-4}$  mpy] and were not shown to be a function of temperature. In 4 M  $MgCl_2$  solution, Titanium Grade 29 showed comparative corrosion resistance as in 1 M NaCl solutions at elevated temperatures. The measured corrosion rates were on the same order as those measured in 1 M NaCl solution, and temperature dependence was also not observed. After the impedance tests, except for mild staining, no corrosion was observed on specimen surface.

The electrochemical impedance spectra for Titanium Grade 7 were also analyzed using the one-time constant circuit model in Figure 2 and the two-time constant circuit model; however, the fitting error was too high to derive any meaningful quantitative corrosion rate data based on the fitting. The spectra were qualitatively compared with those for Titanium Grade 29 under the same test conditions as shown in Figure 4. Except for the slight difference at a higher frequency range, the passive film showed very similar resistance, which suggests very similar corrosion rates under the current test conditions. No significant difference in passive corrosion rates was observed between Titanium Grades 7 and 29 using electrochemical impedance spectroscopy.

During potentiostatic polarization tests for Titanium Grade 29 at 95 °C [203 °F], the anodic current density decreased with time and reached a steady state at approximately 15 days. In 1 M NaCl and 4 M  $MgCl_2$  solutions, the average steady-state anodic current densities were  $1.7 \times 10^{-9}$  and  $1.0 \times 10^{-8}$  A/cm<sup>2</sup> [ $1.6 \times 10^{-6}$  and  $9.4 \times 10^{-6}$  A/ft<sup>2</sup>], respectively, which corresponds to passive corrosion rates of 15 and 89 nm/yr [ $5.8 \times 10^{-4}$  and  $3.5 \times 10^{-3}$  mpy] according to Eq. (4). The anodic current density measured in 1 M NaCl solution for Titanium Grade 29 is similar to that measured previously for Titanium Grade 7 under the same test conditions.<sup>11</sup>

The corrosion rates measured by potentiostatic polarization are about one order of magnitude higher than those measured by electrochemical impedance spectroscopy, possibly resulting from the uncertainty in fitting impedance spectra and the polarization condition used in potentiostatic polarization. The uncertainty in fitting impedance spectra resulting from the high resistive behavior of the titanium passive film could underestimate the corrosion rates; however, the potentiostatic polarization tests could overestimate the corrosion rates. Nevertheless, it appears that electrical chemical impedance provides a lower bound for the corrosion rate, while the potentiostatic polarization rate provides an upper.

## Hydrogen Modeling

The uphill diffusion model was simulated using the implicit finite difference method described previously. The results of these simulations are shown in Figures 5 through

12. As can be seen in the figures, each edge of the weldment reaches a steady-state value, which indicates that the boundary condition did not affect the diffusion simulation. Figures 9 and 10 do not show the hydrogen concentration for the whole length of the weld that was analyzed and only show the central region. This is because the hydrogen concentration reaches a steady state before the edge of the welded material in these simulations. The base corrosion rate used was 58 nm/yr [ $2.3 \times 10^{-3}$  mpy], which is close to that measured using the potentiodynamic polarization method. When two corrosion rates were used, the base corrosion rate was still used for the material with 0 wt% aluminum, while the other materials had a corrosion rate of 3.5 times the base rate [i.e., 203 nm/yr [ $8.0 \times 10^{-3}$  mpy]]. The corrosion rate of the material with aluminum was increased because the material with higher aluminum typically has a higher corrosion rate.<sup>14</sup> By increasing the corrosion rate of the material with aluminum, there will be more hydrogen absorbed in that material, allowing for more hydrogen to diffuse through uphill diffusion.

#### Weld configuration

Figures 5 through 9 show the hydrogen uphill diffusion simulation results for the welding configuration when a titanium alloy with 6 wt% aluminum is welded to a titanium alloy with 0 wt% aluminum. As is shown in these figures, hydrogen will diffuse by uphill diffusion to the alloy with a lower aluminum concentration. The hydrogen concentration under this condition reaches a maximum value of roughly 395 ppm (see Figure 6). This maximum value is located in the metal with the higher aluminum concentration. Figures 10 through 14 show the hydrogen simulation results for the welding configuration when a titanium alloy with 6 wt% aluminum is welded to a titanium alloy with 3 wt% aluminum, and this alloy is welded to a titanium alloy with 0 wt%. These figures show that uphill diffusion will occur at both dissimilar metal intersections. Interestingly, the peak concentration of hydrogen occurs in the transition metal and reaches roughly 405 ppm. However, this increased hydrogen concentration only occurred in the 25 °C [77 °F] simulation. In the 100 °C [212 °F] simulation, the intermediate weld did reduce the maximum hydrogen concentration.

#### Corrosion rate

The enhanced corrosion rate relates to the total amount of absorbed hydrogen in the titanium alloy. By increasing the corrosion rate in the simulation, the hydrogen concentration will be increased in that respective titanium alloy. As expected, the increased corrosion rate leads to an overall increase in the total absorbed hydrogen throughout all of the alloys involved, as shown in Figures 5 through 14. One interesting feature is observed for both the two and three dissimilar metal welds. When the corrosion rates are all equal, the peak hydrogen concentration is located in the 0 wt% titanium alloy as observed in Figures 5, 8, 10, and 13. For the two dissimilar metal weldment, when the corrosion rate is increased in the titanium alloy with the higher aluminum concentration, the peak hydrogen concentration is moved to the other alloy. For the three dissimilar metal welds, when the corrosion rate is increased, the peak hydrogen concentration is moved to the intermediate material, but only at the 25 °C [77 °F] simulation (Figures 11 and 12).

#### Temperature

The main aspect that temperature affects in the uphill hydrogen diffusion (assuming isothermal conditions) is the diffusivity of hydrogen in titanium. By increasing the temperature, the diffusivity increases, enhancing the diffusion process. The results of



the increased temperature are shown in Figures 5 through 14. In the two dissimilar metal welds, the increase in temperature appears to spread the hydrogen concentration throughout the material in the two metal dissimilar weldment simulations. A similar result occurs for the three dissimilar metal weldment. The hydrogen appears to be spread out over the whole model. However, it appears that the increased temperature slightly decreases the concentration of hydrogen observed in the transition alloy, while increasing the overall concentration of hydrogen in the titanium alloy with 0% aluminum. Therefore, at higher temperatures, a transition metal weld material appears to reduce the hydrogen concentration.

## CONCLUSIONS

The goal of this work was to evaluate the hydrogen uphill diffusion along titanium dissimilar metal welds. This was accomplished by examining the uphill diffusion of hydrogen at a titanium boundary between welded materials. Initially, the corrosion rate was measured for Titanium Grades 7 and 29 using both electrochemical impedance spectroscopy and potentiodynamic polarization tests at elevated temperatures. Titanium Grades 7 and 29 were used to simulate titanium alloys with 0 wt% and 6 wt% of aluminum, respectively. No significant difference was observed between the corrosion rates of Titanium Grades 7 and 29 in 1 M NaCl and 4 M MgCl<sub>2</sub> solutions.

An uphill diffusion model was created to examine the hydrogen diffusion along a dissimilar titanium alloy weld line. The measured corrosion rates were used in an uphill diffusion model. Parameters that were evaluated in the uphill diffusion model included weld configuration, corrosion rate, and temperature. Addition of a transition titanium alloy between two dissimilar titanium alloys did reduce the hydrogen concentration, but only at higher temperatures {>100 °C [212 °F]}. At lower temperatures, the transition alloy led to a higher hydrogen concentrations in the transition alloy. By increasing the corrosion rates, there is a higher concentration of hydrogen in the alloy overall, which is what would be expected. Increasing the isothermal temperature leads to a higher diffusivity, which spreads the hydrogen out over all of the welded alloys involved. There did not seem to be a major effect of time, except to allow the corrosion process to continue and deposit more adsorbed hydrogen into the titanium weldment. The location of the maximum hydrogen concentration did not change with time. When a transition titanium alloy is used, higher temperatures decrease the concentration of hydrogen in the transition alloy. Therefore, it would appear that a transition titanium alloy can be used if the temperature is held at an elevated temperature. In fact, the use of a transition weld appears to decrease the hydrogen concentration over an extended period of time if the temperature remains elevated. Therefore, it may be beneficial to use a fillet weld depending upon the application.

## ACKNOWLEDGMENTS

The authors gratefully acknowledge the reviews of Drs. Pavan Shukla and S. Mohanty, the editorial review of L. Mulverhill, and the assistance of J. Gonzalez in the preparation of the manuscript.

This paper describes work performed by the Center for Nuclear Waste Regulatory Analyses (CNWRA<sup>®</sup>) and its contractors for the U.S. Nuclear Regulatory Commission (USNRC) under Contract No. NRC-02-07-006. The activities reported here were

performed on behalf of the USNRC Office of Nuclear Materials Safety and Safeguards, Division of High-Level Waste Repository Safety. This paper is an independent product of the CNWRA and does not necessarily reflect the view or regulatory position of the USNRC.

## REFERENCES

1. Azumi, K., Y. Asada, T. Ueno, M. Seo, and T. Mizuno. "Monitoring Hydrogen Absorption Into Titanium Using Resistometry." *Journal of the Electrochemical Society*. Vol. 149. pp. B422–B427. 2002.
2. Lazzari, L., M. Ormellese, and M. Pedferri. "CP Tests on Hydrogen Embrittlement of Titanium Alloys in Seawater." Proceedings of the 2006 CORROSION Conference. Paper No. 06290. Houston, Texas: NACE. 2006.
3. Hua, F., K. Mon, P. Pasupathi, G. Gordon, and D. Shoesmith. "A Review of Corrosion of Titanium Grade 7 and Other Titanium Alloys in Nuclear Waste Repository Environments." *Corrosion*. Vol. 61. pp. 987–1,003. 2005.
4. Lu, S.C. "Hydrogen Induced Cracking in Titanium Drip Shield of High-Level Waste Repository." UCRL–JC–143999. Livermore, California: Lawrence Livermore National Laboratory. 2001.
5. Kennedy, J.R., P.N. Adler, and H. Margolin. "Effect of Activity Differences on Hydrogen Migration in Dissimilar Titanium Alloy Welds." *Metallurgical Transaction A*. Vol. 24A. pp. 2,763–2,771. 1993.
6. Waisman, J.L., R. Toosky, and G. Sines. "Uphill Diffusion and Progressive Embrittlement: Hydrogen in Titanium." *Metallurgical Transaction A*. Vol. 8A, pp. 1,249–1,256. 1977.
7. Waisman, J.L., G. Sines, and L.B. Robinson. "Diffusion of Hydrogen in Titanium Alloys Due to Composition, Temperature, and Stress Gradients." *Metallurgical Transaction B*. Vol. 4. pp. 291–302. 1973.
8. Pensado, O., D.S. Dunn, G.A. Cragolino, and V. Jain. "Passive Dissolution of Container Materials—Modeling and Experiments." CNWRA 2003-01. San Antonio, Texas: CNWRA. 2002.
9. Dunn, D.S., O. Pensado, Y.-M. Pan, R.T. Pabalan, L. Yang, X. He, and K.T. Chiang. "Passive and Localized Corrosion of Alloy 22—Modeling and Experiments." CNWRA 2005-02, Revision 1. San Antonio, Texas: CNWRA. 2005.
10. Epelboin, I., C. Gabrielli, M. Keddam, and H. Takenouti. "Alternating-Current Impedance Measurements Applied to Corrosion Studies and Corrosion-Rate Determination." *Electrochemical Corrosion Testing ASTM 727*. F. Mansfeld and U. Bertocci, eds. West Conshohocken, Pennsylvania: ASTM International. pp. 150–166. 1981.

11. Brossia, C.S. and G.A. Cragolino. "Effect of Palladium on the Corrosion Behavior of Titanium." *Corrosion Science*. Vol. 46. pp. 1,693–1,711. 2004.
12. ASTM International. "Metals Test Methods and Analytical Procedures." ASTM G102-89 (1999): Standard Practice for Calculation of Corrosion Rates and Related Information from Electrochemical Measurements. Volume 3.02: Wear and Erosion—Metal Corrosion. Published on CD ROM. West Conshohocken, Pennsylvania: ASTM International. 2008.
13. Welty, J.R., C.E. Wicks, and R.E. Wilson. *Fundamentals of Momentum, Heat, and Mass Transfer*. New York City, New York: John Wiley & Sons. 1984.
14. Schutz, R.W. "Performance of Ruthenium-Enhanced Alpha-Beta Titanium Alloys in Aggressive Sour Gas and Geothermal Well Produced-Fluid Brines." Proceedings of the CORROSION '97 Conference. Paper No. 32. Houston, Texas: NACE International. 1997.

**Table 1. Chemical Composition of Titanium Grade 7 and Grade 29 (in Weight Percent)**

Material	Ti*	Pd*	Fe*	C*	N*	O*	H*	Al*	V*	Ru*
Titanium Grade 7 Heat CN2775	Bal	0.16	0.08	0.01	0.01	0.13	0.001	NA	NA	NA
Titanium Grade 29 Heat 00192DB	Bal	NA	0.19	0.04	0.006	0.109	0.0021	5.62	4.16	0.10
*Ti—titanium, Pd—palladium, Fe—iron, C—carbon, N—nitrogen, O—oxygen, H—hydrogen, Al—aluminum, V—vanadium, Ru—ruthenium										

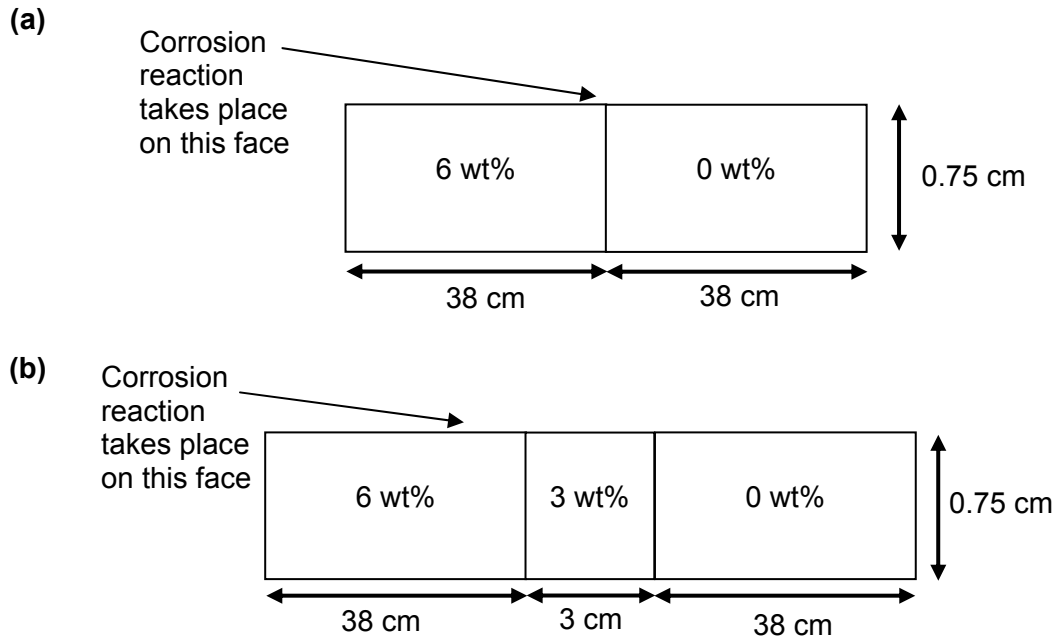


**Figure 1.** Welding configuration examined in the hydrogen model including (a) a two-alloy dissimilar metal weld and (b) a three-alloy dissimilar metal weld

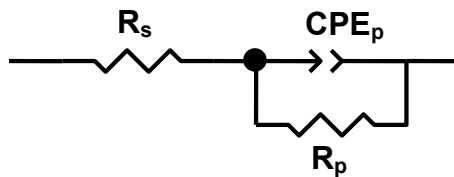


**Figure 2.** One-time constant analog circuit model for fitting electrochemical impedance spectroscopy data

Note: R—Resistance; CPE—Constant Phase Element

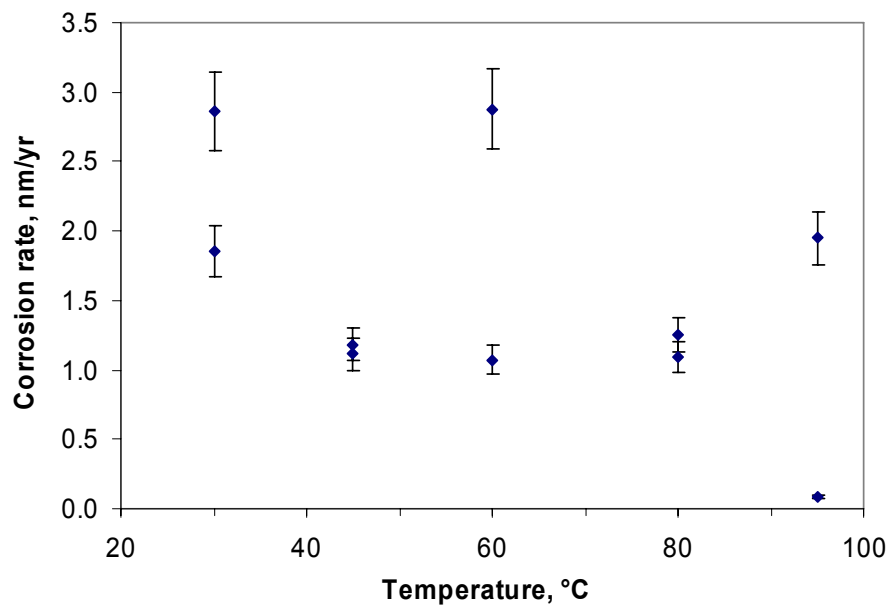


**Figure 3.** Titanium Grade 29 corrosion rates obtained using electrochemical impedance spectroscopy in 1 M NaCl solution at elevated temperatures

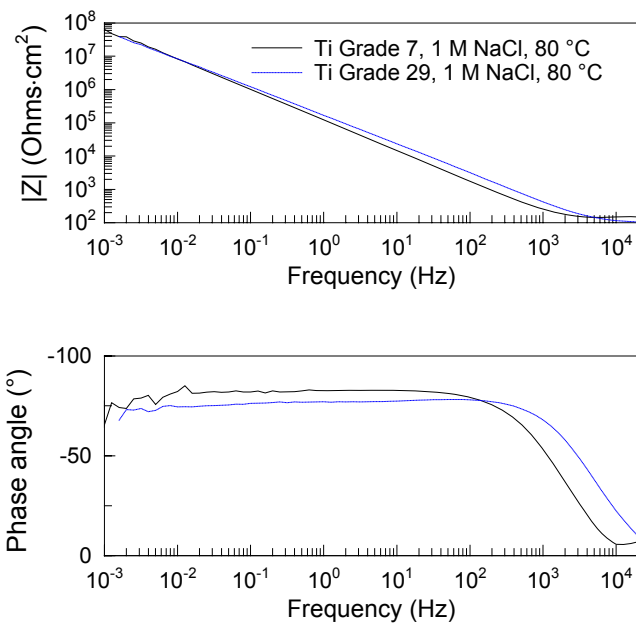


**Figure 4.** Bode plot of the electrochemical impedance spectroscopy of Titanium Grade 7 and Grade 29 in 1 M NaCl at 80 °C [176 °F]

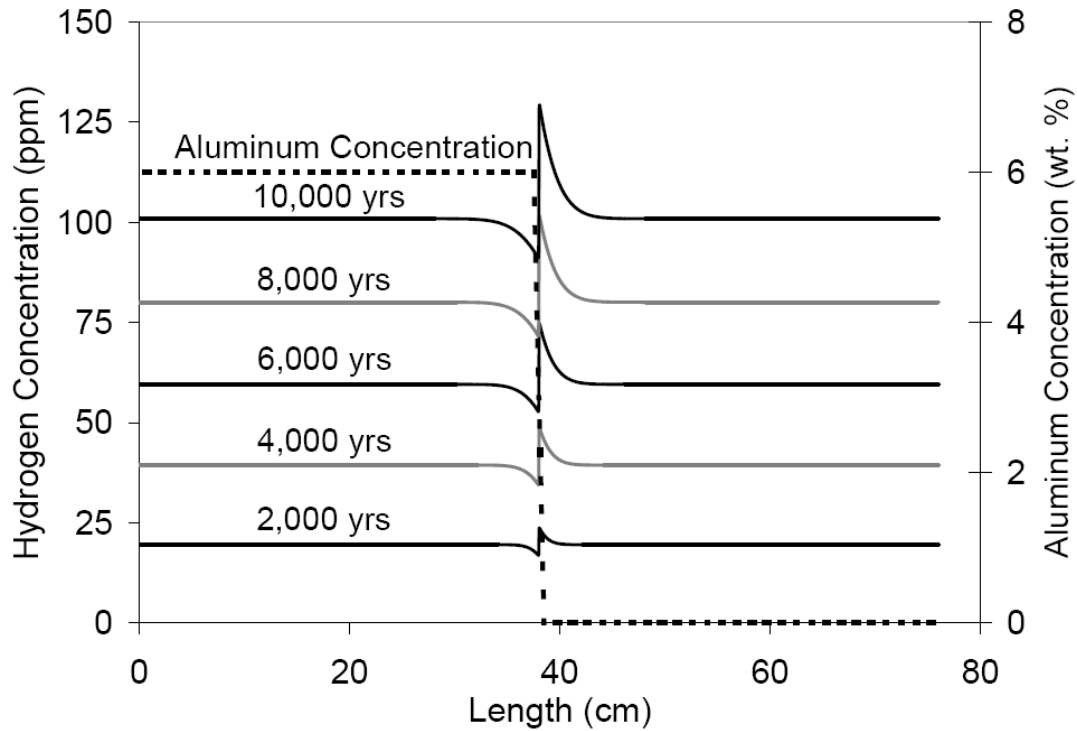


**Figure 5.** Hydrogen concentration in a two dissimilar metal weld at 25 °C [77 °F] with same corrosion rates over 10,000 years

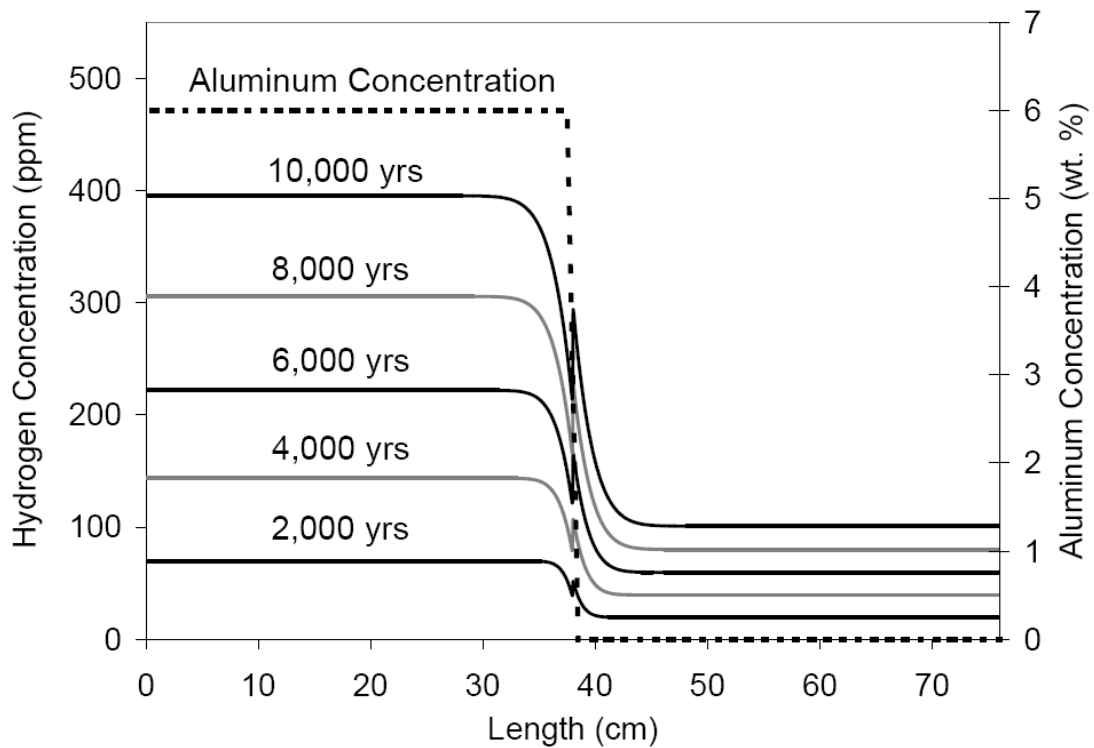


**Figure 6.** Hydrogen concentration in a two dissimilar metal weld at 25 °C [77 °F] with differing corrosion rates over 10,000 years

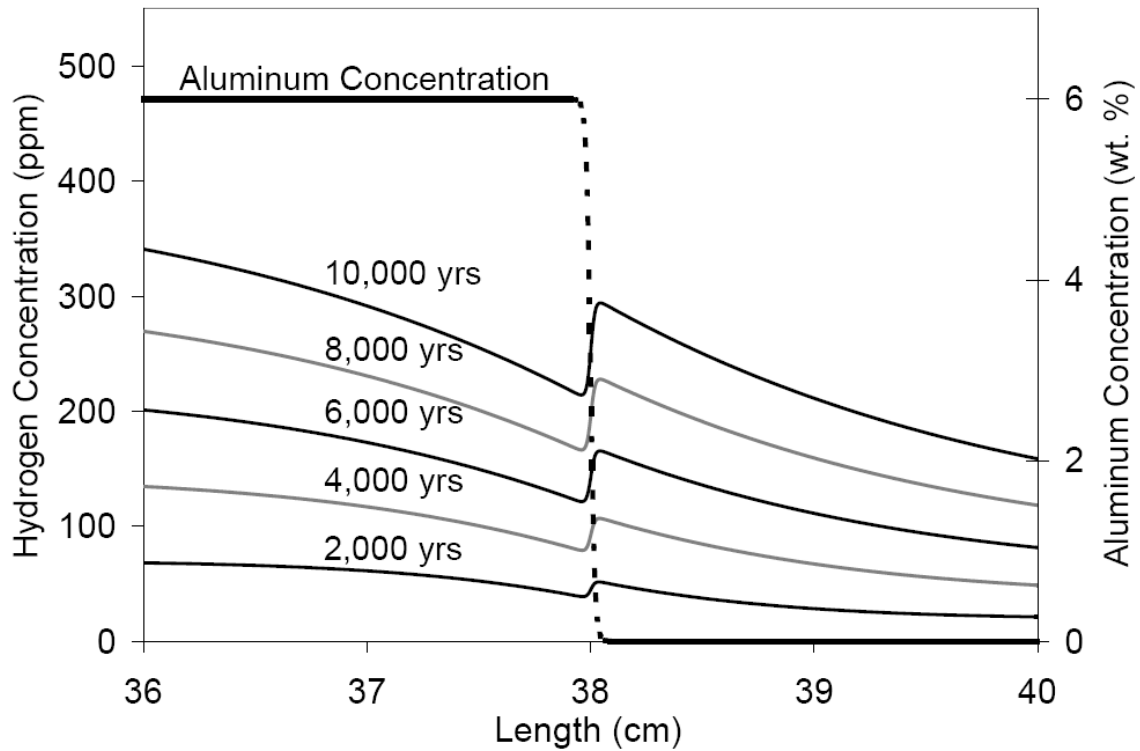


**Figure 7.** Hydrogen concentration in a two dissimilar metal weld at 25 °C [77 °F] with differing corrosion rates over 10,000 years (close up image)

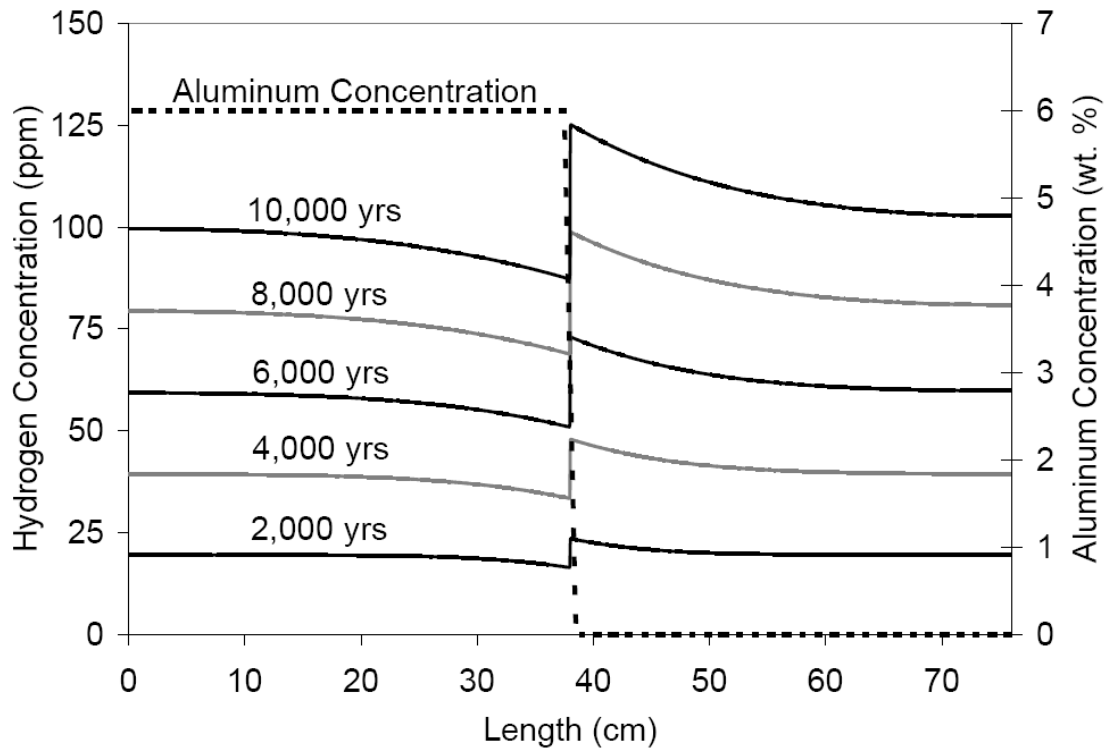


**Figure 8.** Hydrogen concentration in a two dissimilar metal weld at 100 °C [212 °F] with same corrosion rates over 10,000 years

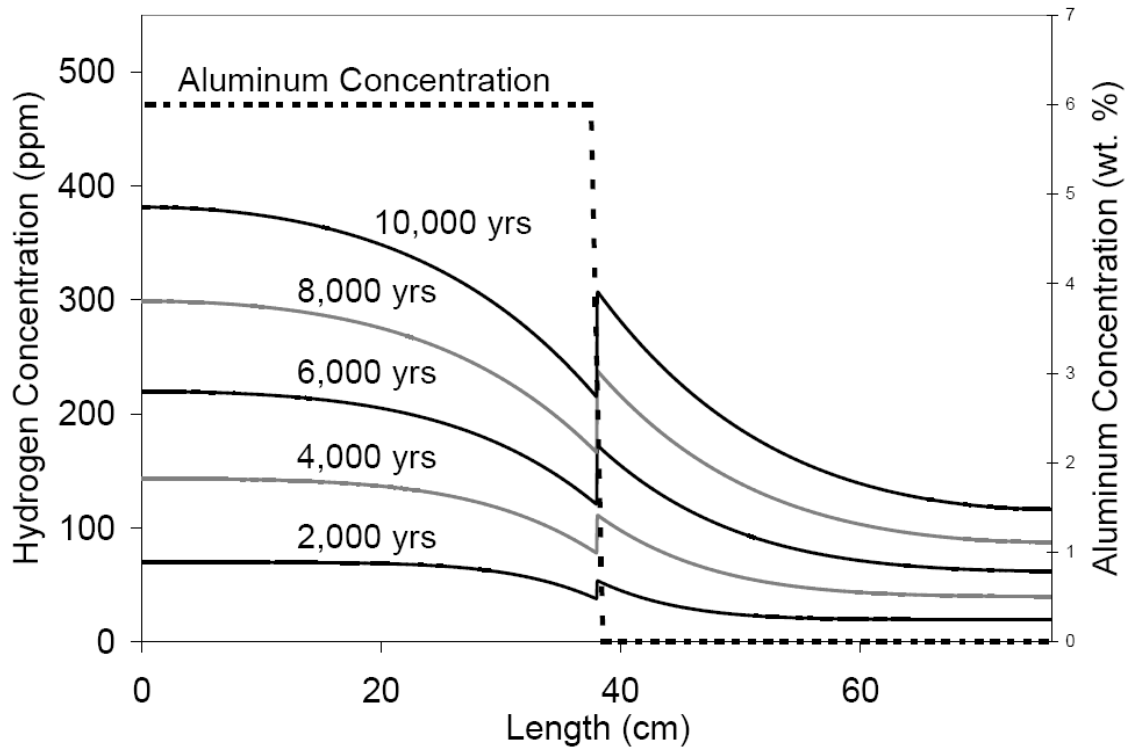


**Figure 9.** Hydrogen concentration in a two dissimilar metal weld at 100 °C [212 °F] with different corrosion rates over 10,000 years

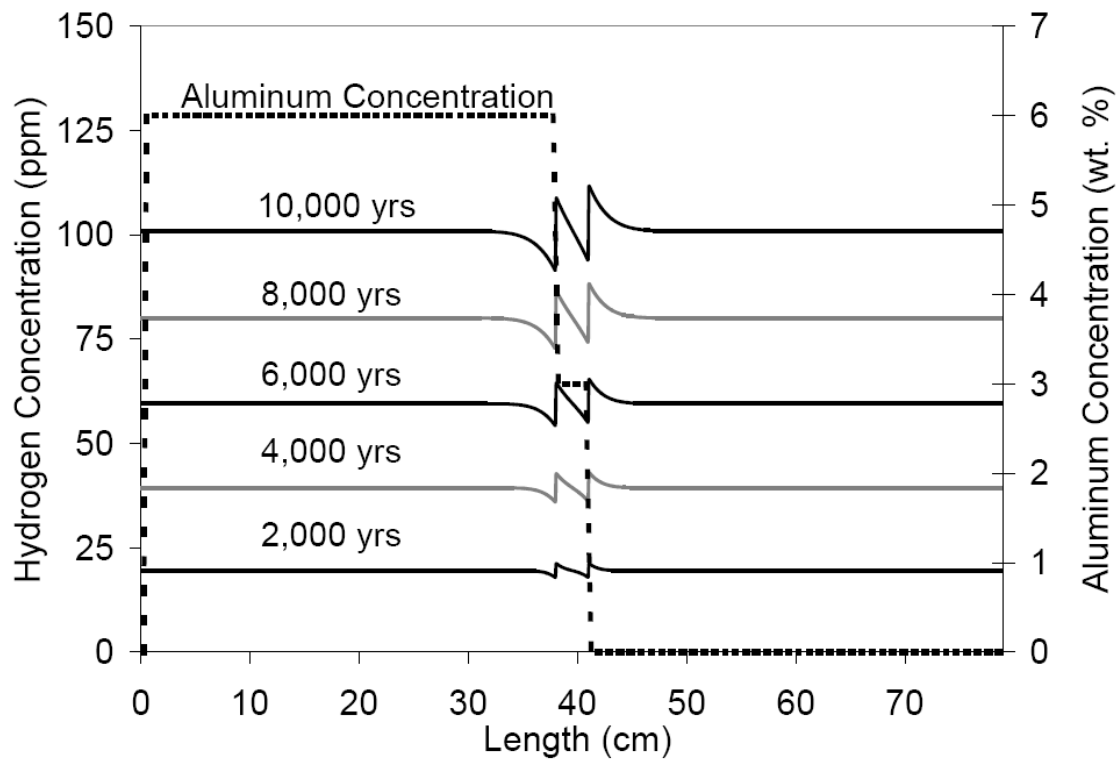


**Figure 10.** Hydrogen concentration in a three dissimilar metal weld at 25 °C [77 °F] with same corrosion rates over 10,000 years



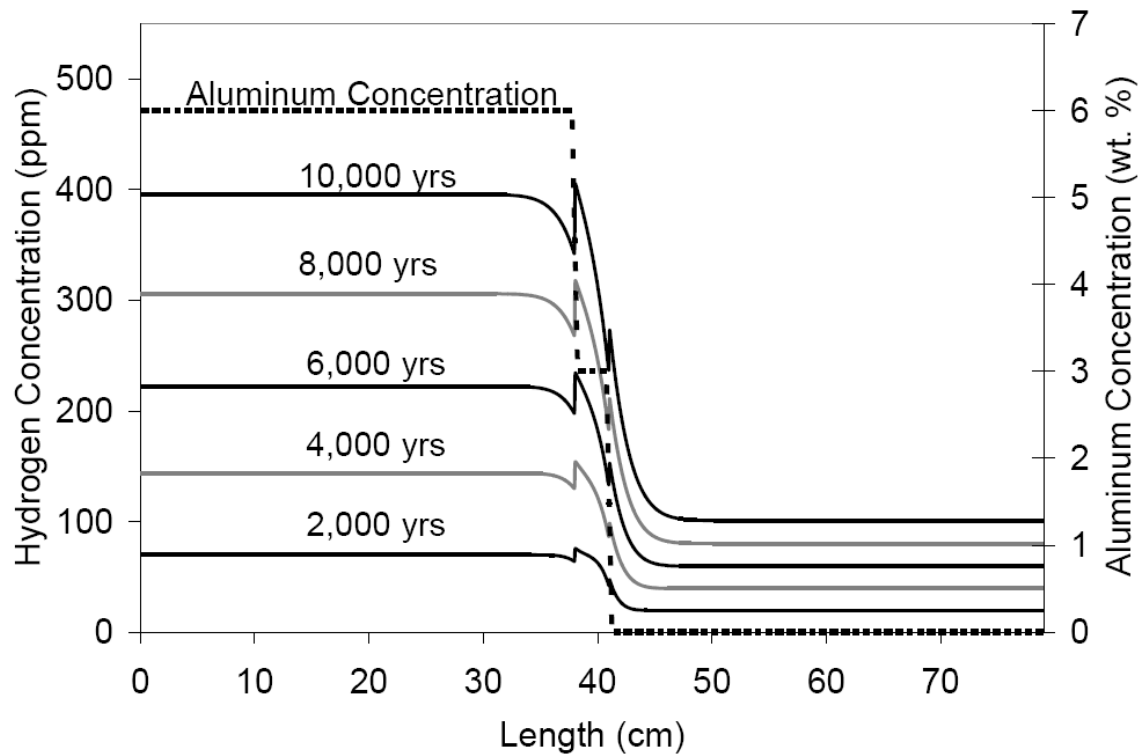


**Figure 11.** Hydrogen concentration in a three dissimilar metal weld at 25 °C [77 °F] with differing corrosion rates over 10,000 years

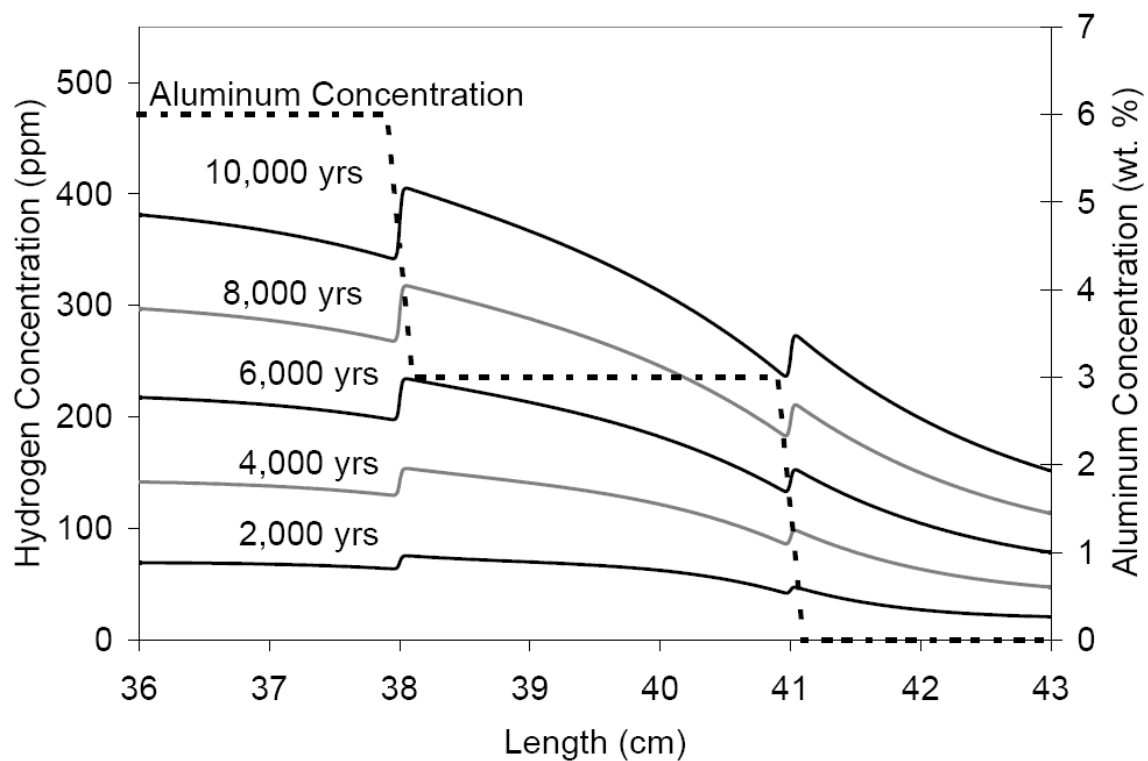


**Figure 12.** Hydrogen concentration in a three dissimilar metal weld at 25 °C [77 °F] with differing corrosion rates over 10,000 years (close up)

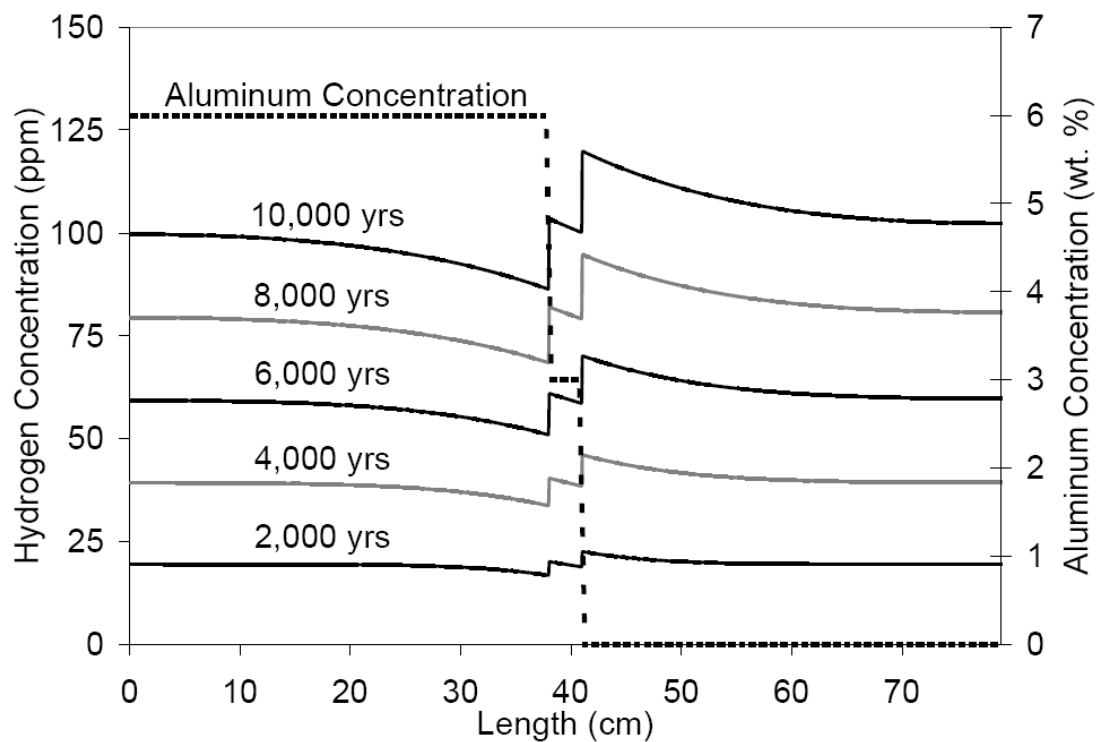


**Figure 13.** Hydrogen concentration in a three dissimilar metal weld at 100 °C [212 °F] with same corrosion rates over 10,000 years

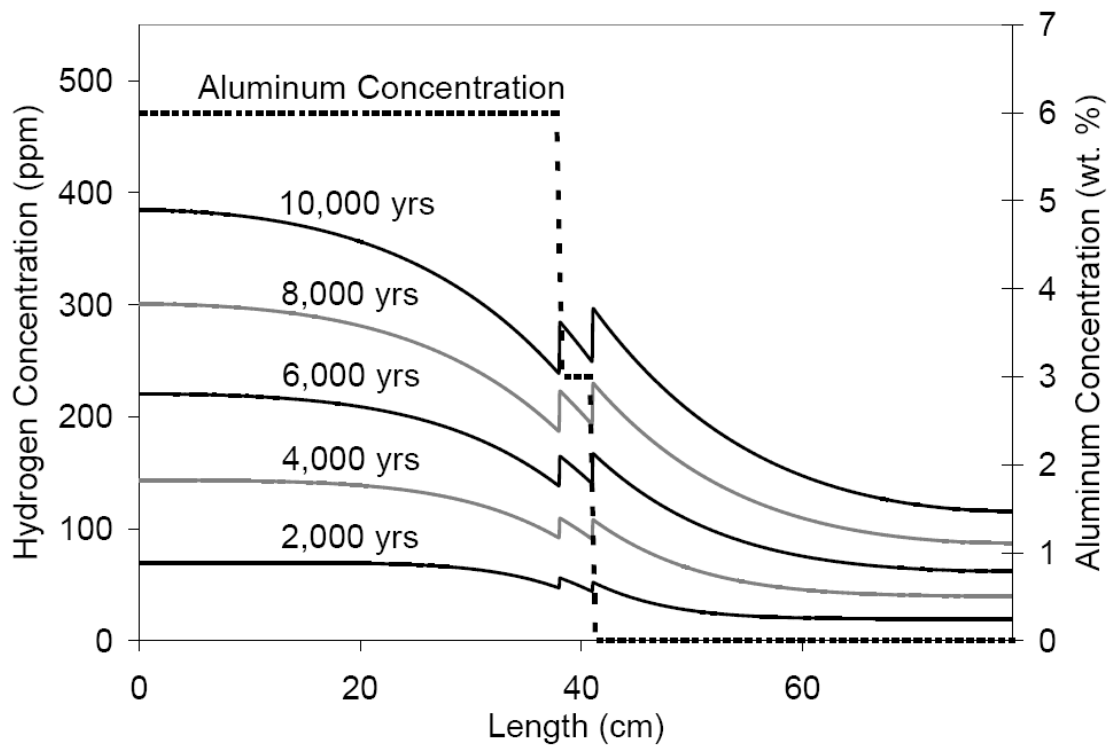


**Figure 14.** Hydrogen concentration in a three dissimilar metal weld at 100 °C [212 °F] with different corrosion rates over 10,000 years